ELSEVIER

Thermochimica Acta 278 (1996) 145–156

thermochimica acta

Modelling of the experimental phenomena occurring during simultaneous TG-DSC measurements of water desorption

K. Sigrist *, H. Stach

Adlershofer Umweltschutztechnik- und Forschungsgesellschaft mbH (AUF), Rudower Chaussee 5, D-12484 Berlin, Germany

Received 24 July 1995; accepted 7 September 1995

Abstract

For the determination of the heat of a given process with a differential scanning calorimeter, it is not only necessary to measure the DSC curve, but also to construct the baseline. If the differential scanning calorimeter is coupled with a balance, the gravimetric measuring values can be used for the construction of the baseline.

In this paper, the model of an input function was calculated from a model equation of the baseline and the gravimetric signal. The corresponding output function results from this together with a model apparatus function by calculation of the convolution integral. Using the regression analysis, the required model coefficients were obtained from the experimental DSC values.

To prove the given model, it was applied to investigations of the desorption process of adsorbed water on zeolites by simultaneous TG-DSC measurements. It was found that with the help of this model, by integration of the corresponding DSC curves, suitable enthalpy values could be obtained even for unfavourable shapes of the baseline.

Keywords: Baseline; DSC; Model; Simultaneous measurements; TG

1. Introduction

In order to determine the heat of a physico-chemical process, e.g. the enthalpy of a transition, adsorption or chemical reaction, by differential scanning calorimetry, it is

* Corresponding author. Leipziger Str. 40, D-10117 Berlin, Germany.

SSDI 0040-6031(95)02732-7

necessary to integrate the corresponding DSC curve between the beginning and ending of the main period. The area between the measured heat flow rate curve and the baseline is equal to the enthalpy of the given process if the calorimeter is calibrated [1–5].

The baseline cannot be measured, but it must be interpolated between the initial and final points of the main period. Often it is possible to approximate the baseline by a straight line between the mentioned points [1], but generally it has a more complicated shape.

In the literature in this field, there are many descriptions of the possible ways to interpolate the baseline for a given problem more correctly [2–10]. A proper classification of the different methods for the construction of the baseline is the following [6]:

(i) Formal methods without physico-chemical justification;
(ii) Methods where physico-chemical assumptions are made, e.g. on the change in the heat capacity during the given process;
(iii) Experimental methods.

The shape of the baseline depends not only on the variation of the heat capacity of the sample, but also on the thermal coupling between the sample and the heat measuring transducer during the observed process as well as on existing heat leaks [1, 3].

The determination of the correct baseline will become particularly difficult if the distance between the initial and the final point is large. Several processes are known that have a base width greater than 300°C, e.g. the desorption of water from Y-zeolites [11]. Another example is shown in Fig. 1. As can be seen in this figure, the water desorption from an NaX-zeolite extends from room temperature to about 400°C, depending on the given conditions.

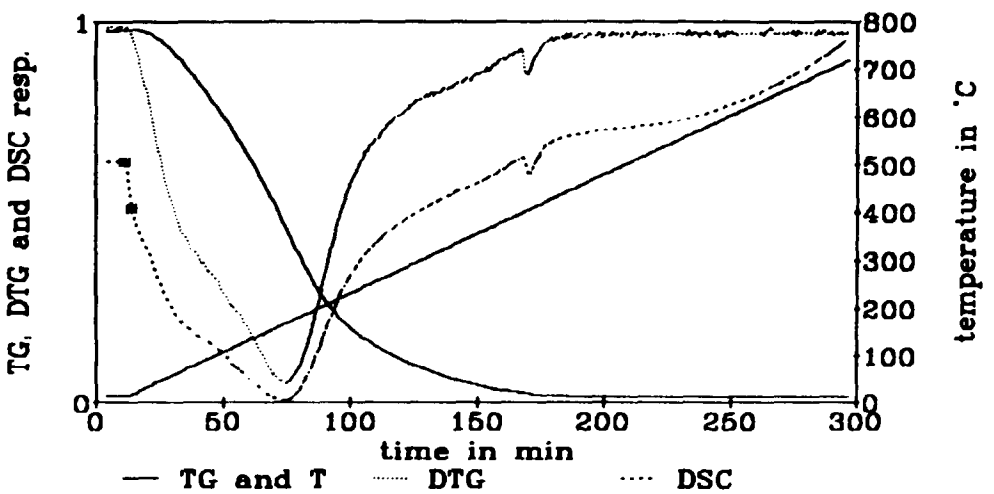

Fig. 1. Simultaneously recorded values during the water desorption from an NaX-zeolite (equipment, Setaram TG-DSC-111; data set A).

However, there is still an additional problem as is also shown in Fig. 1. Because of the unavoidable difference between the heat capacities of the sample and of the reference crucible, the DSC-curve decreases very rapidly when the scanning process starts (see the region between the two points that are marked with *). At about the same time, the desorption process also begins and, consequently, the main calorimetric period.

Generally for the construction of the baseline during the main period, the end part of the initial period can be useful. But that is not possible for the process of water desorption as is shown in Fig. 1 because of the described superposition of the different procedures.

Finally, for the modelling of the baseline and of the heat flow curve, the fact of falsification of the DSC curves by smearing is very important. This means that the output function of the calorimeter depends on both the thermal effect of the sample and the influence of the apparatus.

The different smearing occurrences have been properly investigated in other studies, both from a more theoretical and a more practical point of view [3,4,12–17]. Both the theory of linear response and desmearing using Green's functions [12–16], and the desmearing procedures using Tian's equation and by solving the convolution integral [3,4,17], have special importance.

The description of output DSC curves by the method of convolution is of particular interest for this paper. It assumes that the output function is equal to the convolution integral of the input function generated from the sample, and of the apparatus function. Generally, the latter is determined experimentally by additionial measurements of special heating effects, e.g. by very fast passing transitions or by short light pulses.

The aim of this paper is to describe DSC curves by using model equations of the baseline and the apparatus function. In order to obtain the required coefficients in these equations it is necessary to have both the DSC measuring data, and also unsmeared and simultaneously measured values which are independent of the DSC curve. Such data can be obtained from TG measurements.

2. The modelling of the apparatus function

As mentioned in the previous section the apparatus function is usually a sequence of experimental points. But for the modelling it is necessary, or at the very least very helpful, to find an analytical expression, if an appropriate approximation for the apparatus function could be given.

As an empirical formula for such an approximation of the apparatus function, a relation of the following form is imaginable

$$g(t) = \frac{a^{n+1}}{n!} \cdot t^n \cdot \exp(-at) \tag{1}$$

where t is time, a is the apparatus constant, and $n = 0, 1, 2 \ldots$ is an integer constant.

By integrating $g(t)$ between $t = 0$ and $t = \infty$, it can be seen that the area below this curve is equal to 1, as must be supposed for the desired aim.

The suitability of Eq.(1) as a model for the apparatus function was tested experimentally. A simple example of such a test is shown in Fig. 2. Here the DSC curve of fusion of KSCN crystals is plotted (see the experimental values). As can be seen, the base distance of this transition is very small in comparison with its extent for the desorption process shown in Fig. 1; under the given experimental conditions, the baseline seems approximate to a horizontal line. For this example, there are no problems in the determination of the input function.

The shape of the input function in Fig. 2 resembles a triangle. This can be explained as follows. So long as no additional event occurs in the sample, a certain quantity of heat flows permanently from around the sample into the sample during the temperature scanning. The temperature of the sample increases. Nevertheless the DSC curve has a certain level (initial period). When the melting point is attained, the temperature of the sample no longer increases, but remains constant because the heat from around the sample is needed for the melting process. The melting rate depends on the heat flow into the sample and this increases as a result of the difference in the temperature between the sample and its surroundings. At the end of the fusion, the input function suddenly drops to zero (end of the main period and beginning of the final period) and the temperature of the sample shifts to the same value as its surroundings.This input function can be expressed by

$$f(t) = 0; \quad \text{if} \quad t_B \geq t \geq t_E$$

or

$$f(t) = b(t - t_B); \quad \text{if} \quad t_B \leq t \leq t_E \tag{2}$$

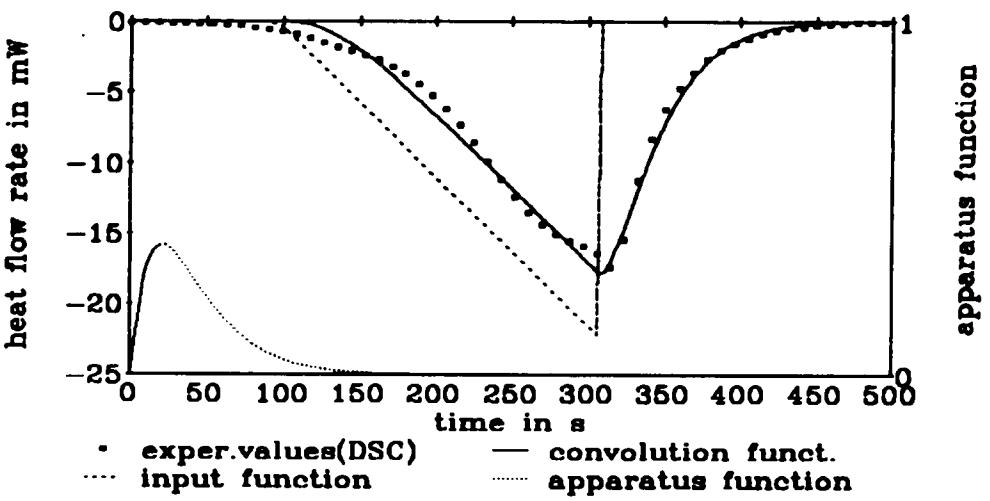

Fig. 2. DSC curve for the fusion process of KSCN crystal powder (for conditions see No. 2 in Table 1) and corresponding model curves.

where

$$b = -\frac{2A}{(t_E - t_B)^2}$$

where A is peak area, and t_B and t_E the time at the beginning and ending of the main period, respectively.

Finally, the output function is equal to the convolution integral

$$\phi = \int_{\tau=0}^{\tau=t} f(\tau) \cdot g(t-\tau) \cdot d\tau \tag{3}$$

The curves for $\phi(t)$, $g(t)$ and $f(t)$ in Fig. 2 result with $n = 1$ and with those constants a, t_B and t_E (see Eqs.(1) and (2)), which are obtained by regression analysis for $\phi(t)$ from the experimental values.

As can be seen from Fig. 2, the model Eqs. (1)–(3) appropriately describe the experimental curve. The deviation of the calculation from the experimentally measured peak area amounts to about 0.24% for this example.

Additional melting tests were made for further verifications of the apparatus model equations. The substances used and the measuring conditions can be seen in Table 1.

The nearness of the calculated to the experimentally measured DSC values depends not only on the measuring conditions, but also on the assumed integer constant n because of its influence on the shape of the model function $g(t)$. Both influences (the measuring conditions and the magnitude of the constant n) on the deviations of the calculated from the experimentally measured DSC peak areas are shown in Table 2.

As can be seen from Table 2, the influences of the test conditions and of the assumed constant n on the named deviations are mostly small, but not systematic. Therefore, it is difficult to find the best n for all conditions. But it seems to be a good compromise to choose $n = 1$, and so this value will be used in all the following calculations.

If n is determined, the model apparatus function $g(t)$ depends only on a single parameter, the apparatus constant a. The results of the calculation of a (using the

Table 1
Substances and conditions for the tests of the melting process

No.	Substance	Heating rate/°C min^{-1}	Temperature interval/°C
1	KSCN	1	165–183
2	KSCN	2	162–187
3	KSCN	5	154–214
4	$AgNO_3$	1	196–220
5	$AgNO_3$	2	196–220
6	$AgNO_3$	5	189–248
7	KNO_3	1	328–339
8	KNO_3	2	329–342
9	KNO_3	5	326–350

Table 2
Relative deviations (in %) of calculated and measured DSC values in dependence on the assumed integer constant n

No.[a]	$n=0$	$n=1$	$n=2$	$n=3$	$n=4$
1	0.19	0.21	0.23	0.24	0.24
2	0.21	0.24	0.25	0.26	0.26
3	0.26	0.25	0.29	0.31	0.32
4	0.29	0.34	0.36	0.37	0.37
5	0.27	0.28	0.30	0.32	0.33
6	0.42	0.42	0.43	0.46	0.48
7	0.26	0.18	0.20	0.21	0.22
8	0.40	0.23	0.26	0.28	0.29
9	0.61	0.47	0.41	0.38	0.36

[a] For the No. see Table 1.

Table 3
Apparatus constant a in s^{-1} (calculated with $n=1$) for various conditions (see melting process Nos. 1–9 in Table 1)

T_B/°C[a]	Substance (process No.)	a/s^{-1} for heating rate			a_T/s^{-1}[b]
		1°C min^{-1}	2°C min^{-1}	5°C min^{-1}	
172	KSCN (1, 2, 3)	0.0445	0.0470	0.0497	0.0471
207	$AgNO_3$ (4, 5, 6)	0.0386	0.0482	0.0492	0.0453
332	KNO_3 (7, 8, 9)	0.0522	0.0547	0.0514	0.0528
a_R/s^{-1}[b]		0.0451	0.0500	0.0501	

[a] Temperature at $t=t_B$ (see Eq. (2)).
[b] Mean values of the apparatus constant, averaged with respect to the temperature and heating rate, respectively.

regression analysis from the experimental values) are listed in Table 3. The average apparatus constants a_R in Table 3 increase only with the rise in the heating rate. But a_T depends apparently on more than one variable: on the temperature and on the nature of the substance.

Thus altogether, for the application of Eq. (1) to some given DSC investigation and the determination of the apparatus constant, not only the measuring conditions must be taken into account, but also the properties of the given substance.

3. The modelling of the baseline and the DSC curve

3.1. The basic shape of the baseline

As long as no exothermic or endothermic processes take place in the sample, the following differential equation (see Eqs. (5.15) and (5.16) in Ref. [3]) is approximately valid for a heat flow differential scanning calorimeter

$$\phi_{OS} - \phi_{OR} = (C_S - C_R)\cdot\frac{dT_R}{dt} - RC_S\frac{d(\phi_{OS} - \phi_{OR})}{dt} \tag{4}$$

where O, S and R in the indices indicate the oven, sample and reference crucible, respectively, and ϕ, C, T, R and t denote the heat flow, heat capacity, temperature, heat resistance and time, respectively.

During the scanning period the heating rate (dT_R/dt) is constant. If it is combined with C_S, C_R and R to form a coefficient B, and a coefficient A is obtained by combining C_S with R, Eq. (4) can be rewritten

$$\frac{d\phi_{SR}}{dt} + A\cdot\phi_{SR} = B \tag{5}$$

defining $\phi_{SR} = \phi_{OS} - \phi_{OR}$.

For a first approximation, we can assume that A and B are constant. But in general, especially for a large base distance, we cannot forget that A and B both depend on the temperature and therefore also on the time. An exact formulation of the dependence of A or B on t is difficult. It is hindered, because:

(i) Real interest is in the application of Eq. (5) to processes in which the heat capacity is changed by the production of another substance, e.g. by reaction or transition; and
(ii) The source Eq.(4) is only an approximation which neglects other influences.

As will later be proved in Section 3.3, a simple empirical form of Eq. (5) can be successful when applied to experimental systems. This form corresponds to the use of a constant for A and of a series expansion for B

$$B = B_0 + B_1 t + B_2 t^2 + \ldots \tag{6}$$

Thus, the solution of the differential equation (5) is

$$\phi_{SR} = c\cdot\exp(-At) + b_0 + b_1 t + b_2 t^2 + \ldots \tag{7}$$

where c is the constant of integration, and the b_i values result, as can be shown, by combining A and the B_i, e.g.

$$b_0 = \frac{B_0}{A} - \frac{B_1}{A^2} + 2\frac{B_2}{A^3} - + \ldots \tag{7a}$$

Eq. (7) describes the input function of the baseline. It does not take into account the smearing from the influence of the apparatus.

3.2. The DSC input function

The following relates to the coupling of calorimetric with gravimetric measurements in the same equipment. This is generally only used to compare the different results of both methods. But in this paper the gravimetric measurements will be used directly to obtain better results from the calorimetric measurements.

The method of simultaneous TG-DSC allows us to measure both sorts of values, DSC and TG, in dependence on the time. From the thermogravimetric values, it is also easy to obtain the DTG data. Thus, if during the heating period a process proceeds with a variation in the sample mass, correlations are given as shown in Fig. 1 . The similarity of the DSC and DTG curves is obvious. This is very understandable, because the corresponding DSC input function is given (using Eq. (7)) by

$$f(t) = c \cdot \exp(-At) + h\frac{\mathrm{d}m}{\mathrm{d}t} + b_0 + b_1 t + b_2 t^2 + \ldots \tag{8}$$

where m is the mass of the sample and h the enthalpy of the process in relation to the unit of mass. The derivative $(\mathrm{d}m/\mathrm{d}t)$ corresponds to the DTG curve.

Generally the enthalpy is not constant. When applied to the desorption processes, h corresponds, for example, to the desorption enthalpy and is therefore a function of the temperature and of the sample mass. During the scanning period, both are functions of time. Thus, it follows that $h = h(t)$. It is possible to approximate this dependence with a series expansion with respect to t at the point $t = t_m$

$$h = h_0 + h_1(t - t_m) + h_2(t - t_m)^2 + h_3(t - t_m)^3 + \ldots \tag{9}$$

A useful choice of t_m is the time at which the loss of the sample mass has its mean value.

Substituting h from Eq. (9) into Eq. (8), the DSC input function $f(t)$ can be obtained, and this is used in the following.

3.3. The DSC output function

Using the input function $f(t)$ from the previous section and the same apparatus function as in Section 2 (see Eq. (1) for $n = 1$), the output function is given by the convolution integral Eq. (3). This is the desired model equation.

The application of the given model to real systems is of particular interest. To achieve this, investigations of the desorption process of adsorbed water on zeolites were carried out, using the TG-DSC-111 (Setaram).

Series expansions were used with truncation after the last terms given in Eqs. (8) and (9), respectively, for which it is necessary to determine the coefficients c, A, b_0, b_1, b_2, h_0, h_1, h_2, h_3 and the apparatus constant a by regression analysis of the experimental values.

At first, b_0 can be eliminated by a suitable moving of the origin. If the starting point corresponds to the second, with a * marked point in Fig. 1, a DSC peak as shown in Fig. 3 results. Fig. 3 will be used to give an example of the suitability of the model

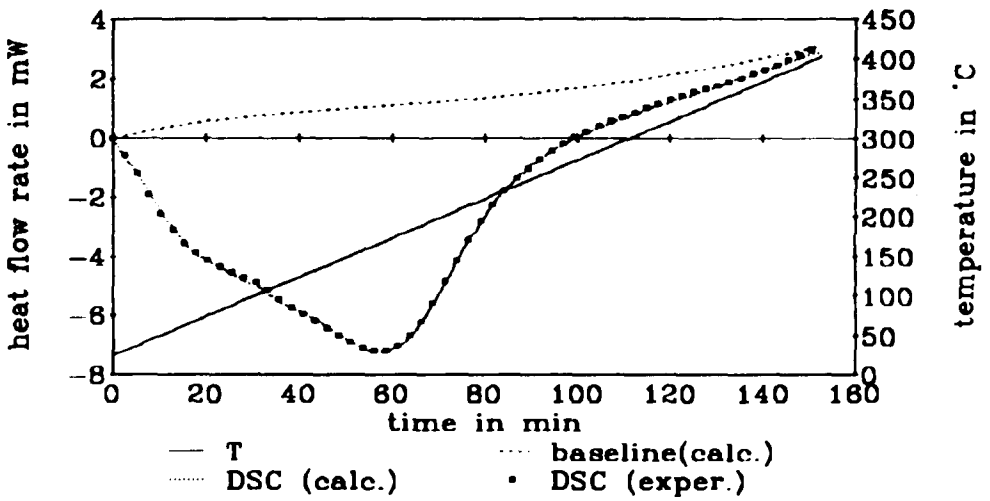

Fig. 3. Recorded and calculated DSC values and calculated baseline for the water desorption from an NaX-zeolite (data set A).

proposed. The calculated values of the heat flow are plotted among other curves and, as can be seen, the calculated heat flow curve accurately approaches the experimentally measured values.

Finally, the calculated baseline is shown in Fig. 3. Its shape is not very different from a straight line because of the favourable conditions of the given measurement.

It is possible to determine the apparatus constant a for each measured data set with the described method. But in general it would be better if, first, the average apparatus constant is calculated from numerous data sets and then, using this mean value, the rest of the coefficients of each set are calculated by a second regression analysis.

The results of the first step are given for 31 data sets of powdered zeolites and for 22 data sets of granulated zeolites in Table 4. The apparatus constant is also given in Table 4, which was obtained for the fusion process of KSCN, determined by the method of Section 2.

Table 4
Average apparatus constant and confidence interval (at $P = 0.95$) for water desorption from different formed zeolite samples and for fusion of KSCN (reference system) under similar conditions

Sample	Conditions		
	Heating rate/°C min^{-1}	Temperature/°C	Apparatus constant a/s^{-1}
Zeolite powder	2.5	152[a]	0.0264 ± 0.0038
Zeolite granules	2.5	149[a]	0.0345 ± 0.0055
KSCN	2.5[a]	172	0.0471 ± 0.0034

[a] Mean value.

The apparatus constant should only depend on the heat flow into the sample and on several other properties of the apparatus. Therefore, it should be a constant for various samples, if the temperature is constant. But as shown in Table 4, the values of the apparatus constant are different for the different substances and processes, respectively (a significant difference is verified by the t-test at $P = 0.95$).

The causes of this discrepancy are not only the use of the mean values of the desorption temperature, averaged for an interval of more than 300°C, e.g. see Fig. 1, but probably also certain influences of the sample properties, e.g. the heat conductivity [12]. For these reasons it would be best if the apparatus constant were determined possibly for the same substance, process and measuring conditions as the measurements for the determination of the other coefficients (see Section 2).

The most important measurement in our desorption investigations was the desorption enthalpy h, especially h_0, i.e. h at $t = t_m$ (see Eq. (9)). In the following we shall investigate whether the measuring conditions have an influence on this quantity.

Several measuring conditions for 3 selected data sets (from a series of 7) are listed in Table 5. The chosen conditions were the sample mass and the individual properties of the heat-flow measuring transducers used. The latter were characterized quantitatively with the corresponding baseline drift after 150 min from the beginning of the temperature scanning. The enthalpy values h_0 are also shown in Table 5.

As can be seen in Table 5, there are considerable differences in the conditions but no significant differences for h_0 regarding a confidence interval with $P = 0.95$. This is surprising, particularly because the transducer for data set C was damaged. Therefore the influence of the mentioned conditions on the calorimetric results shall be discussed in detail, including Figs. 3 and 4.

Comparing first the data sets A and B, it follows from the corresponding Figs. 3 and 4, respectively, that:

(i) The peak areas between the baseline and the DSC curve for sets A and B are equivalent to the different sample masses of 50 and 25 mg, respectively. Therefore, it is understandable that the desorption enthalpies per unit of mass loss are the same, and so are the h_0 values in Table 5.

Table 5
Several measuring conditions and the desorption enthalpy h_0 of 3 selected data sets[a] for the desorption of water from NaX powder[b]

Data set	Sample mass/mg	Heat-flow measuring transducer	Baseline drift/mW	Desorption enthalpy h_0 J (g $(H_2O)^{-1}$
A	50	1	3.1	3030
B	25	2	6.6	3060
C	25	2[c]	12.5	2880

[a] From a series of 7 data sets with h_0 (J g^{-1}) = 2980 ± 100 ($P = 0.95$).
[b] Heating rate, 2.5°C min^{-1}; gas flow rate and gas, 1.0 l h^{-1} (N_2).
[c] Transducer 2 after a damage, generating a "heat leak" between the DSC tube and the thermocouples.

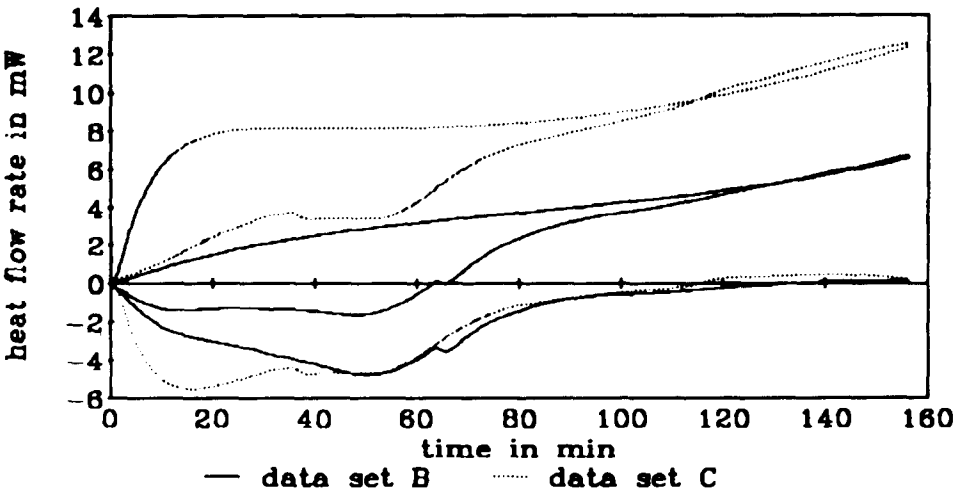

Fig. 4. Heat flow rate (middle), baseline (above) and difference of both (below) for two data sets, measured during the water desorption from an NaX-zeolite.

(ii) The shapes of both the baselines and both the DSC curves, respectively, are similar for sets A and B, although the heat-measuring transducers and the corresponding baseline drifts were different.

Fig. 4 shows the results when data set B is compared with data set C:

(i) The shape of the baselines on the one hand and of the DSC curves on the other are clearly different for sets B and C, because the transducer for set C was damaged.

(ii) The two data sets become more similar if we compare the difference curves establishing the difference between the heat flow and baseline curves (see the analogous difference between Eqs. (8) and (7)). Both of these difference curves are nearly the same at the time $t = 52$ min. This time corresponds to t_m and so the ordinates at this point correspond to the h_0 values. Both are equal to each other because the sample masses are the same for sets B and C (see Table 5).

(iii) The difference curve for set C deviates from that for data set B, especially if t is smaller than about 35 min. This region is beyond the limits of validity of the model in the given approximation.

4. Conclusions

The model presented adequately describes the experimental phenomena occurring during the given simultaneous TG-DSC measurements, if the measuring conditions are acceptable.

Using this model, it is possible to obtain suitable enthalpy values by integrating the corresponding DSC curves even for an unfavourable shape of the baseline.

Unfavourable conditions can result from the coupling of the differential scanning calorimeter with the balance, because for the balance to be usable, a mechanical contact between the sample and the DSC tube must be avoided and therefore the corresponding thermal coupling is relatively bad. Using the model offered, it is possible to compensate this unfavourable influence.

Acknowledgments

The authors thank the Bundesministerium für Bildung und Forschung for financial support. In addition, they greatly appreciate the helpful discussions of Dr. D. Schultze (Bundesanstalt für Materialforschung und -prüfung, Berlin) and Dr. K.-H. Radeke (Institut für Technologie und Umweltschutz e.V., Berlin) on the thermoanalytical measurements and the theoretical interpretation of the measured curves.

References

[1] S.M. Sarge, E. Gmelin, G.W.H. Höhne, H.K. Cammenga, W. Hemminger and W. Eysel, Thermochim. Acta, 247 (1994) 129–168.
[2] J.H. Flynn, Thermochim. Acta, 217 (1993) 129–149.
[3] W.F. Hemminger and H.K. Cammenga, Methoden der Thermischen Analyse, Springer-Verlag, Berlin, 1989.
[4] W.F. Hemminger and G.W.H. Höhne, Calorimetry—Fundamentals and Practice, VCH Verlags-Gesellschaft, Weinheim, 1984.
[5] W.W. Wendlandt, Thermal Analysis, John Wiley & Sons, New York, 1986.
[6] W.F. Hemminger and S.M. Sarge, J. Therm. Anal., 37 (1991) 1455–1477.
[7] K. Sigrist, Thermochim. Acta, 42 (1980) 333–341.
[8] J.S. Crighton and F.W. Wilburn, Thermochim. Acta, 203 (1992) 1–5.
[9] F.W. Wilburn, R.M. McIntosh and A. Turnock, Trans. J. Br. Ceram. Soc., 73 (1974) 117–123.
[10] A. Sanahuja, Thermochim. Acta, 90 (1985) 9–14.
[11] E. Trif, D. Strugaru, I. Ivan, R. Russu, G. Gheorghe and A. Nicula, J. Therm. Anal., 41 (1994) 871–880.
[12] J. Schawe and C. Schick, Thermochim. Acta, 187 (1991) 335–349.
[13] G.W.H. Höhne and J.E.K. Schawe, Thermochim. Acta, 229 (1993) 27–36.
[14] J.E.K. Schawe, C. Schick and G.W.H. Höhne, Thermochim. Acta, 229 (1993) 37–52.
[15] J.E.K. Schawe, G.W.H. Höhne and C. Schick, Thermochim. Acta, 244 (1994) 33–48.
[16] J.E.K. Schawe, C. Schick and G.W.H. Höhne, Thermochim. Acta, 244 (1994) 49–59.
[17] U. Ulbrich and H.K. Cammenga, Thermochim. Acta, 229 (1993) 53–67.